Title
Diurnal trends of indoor and outdoor fluorescent biological aerosol particles in a tropical urban area

ISBN
9781713823605

Authors
Li, Jiayu
Zuraimi, Sultan
Schiavon, Stefano
et al.

Publication Date
2022-11-01

DOI
10.1016/j.scitotenv.2022.157811

Peer reviewed

Diurnal trends of indoor and outdoor fluorescent biological aerosol particles in a tropical urban area

Jiayu Li[*,†], Sultan Zuraimi[†], Stefano Schiavon[‡], Man Pun Wan[§], Jinwen Xiong[§], Kwok Wai Tham[‖]

[†]Berkeley Education Alliance for Research in Singapore (BEARS), 1 Create Way, 138602, Singapore

[‡]Center for the Built Environment (CBE), UC Berkeley, 390 Wurster Hall, Berkeley, CA, 94720, USA

[§]School of Mechanical and Aerospace Engineering, Nanyang Technological University, 50 Nanyang Ave, 639798, Singapore

[‖]Department of Building, National University of Singapore, 4 Architecture Drive, 117566, Singapore

* Corresponding Author:

Jiayu Li (ORCID: 0000-0002-5398-1151)

Address: 1 Create Way, #11-02 Create Tower, Singapore 138602

E-mail: jiayu.li@berkeley.edu; jiayuliaq@gmail.com

Abstract: We evaluated diurnal trends of size-resolved indoor and outdoor fluorescent biological airborne particles (FBAPs) and their contributions to particulate matter (PM) within 0.5–20 μm. After a ten-week continuous sampling via two identical wideband integrated bioaerosol sensors, we found that both indoor and outdoor diurnal trends of PM were driven by its bioaerosol component. Outdoors, the median [interquartile range] FBAP mass concentration peaked at 8.2 [5.8–9.9] μg/m^3 around sunrise and showed a downtrend from 6:00 to 18:00 during the daytime and an uptrend during the night. The nighttime FBAP level was 1.8 [1.4–2.2] times higher than that during the daytime, and FBAPs accounted for 45% and 56% of PM during daytime and nighttime, respectively. Indoors, the rise in concentrations of FBAPs smaller than 1 μm coincided with the starting operation of the heating, ventilation, and air conditioning (HVAC) system at 6:00, and the concentration peaked at 8:00 and dropped to the daily average by noontime. This indicated that the starting operation of the HVAC system dislodged the overnight settled and accumulated fine bioaerosols into the indoor environment. For particles larger than 1 μm, the variation of mass concentration was driven by occupancy. Based on regression modeling, the contributions of indoor PM, non-FBAP, and FBAP sources to indoor mass concentrations were estimated to be 93%, 67%, and 97% during the occupied period.

Keywords: bioaerosols; particulate matter; aerosol compositions; human exposure; air quality; WIBS

1 INTRODUCTION

Bioaerosols, representing up to 15–68% of atmospheric particulate matters (PM) by mass or number in different locations and environments (Jaenicke, 2005; Marcovecchio and Perrino, 2021; Morris et al., 2011; Pöschl et al., 2010), are of high interest due to their exposure effects on human health (Kim et al., 2018; Morawska et al., 2017; Schwartz and Collins, 2007; Shiraiwa et al., 2017) and their important role in climate and atmospheric science (Després et al., 2012; Huang et al., 2021; Pöschl et al., 2010).

Globally, the level of atmospheric fine PM with a diameter less than 2.5 μm ($PM_{2.5}$) varies in a certain trend diurnally (Manning et al., 2018). In many cities, the nighttime $PM_{2.5}$ level will be higher than that during the daytime, especially when the anthropogenic emissions are not strong or when the diurnal cycle of atmospheric mixing dominates. A study focused on bioaerosols in the tropics (Gusareva et al., 2019) showed that the level of airborne microorganisms follows a clear diurnal pattern. This pattern was assumed to be affected by environmental factors, such as temperature, humidity, and the concentration of carbon dioxide. Bioaerosols in the daytime showed higher diversity but contained less biomass than those in the nighttime. The two studies mentioned above did not explore the relationship between PM and bioaerosol. Further, no studies have provided size-resolved aerosol information on the diurnal trend indoors and outdoors in the tropics, which is essential to further understand human exposure and their health impacts (Harrison and Yin, 2000; Kelly and Fussell, 2012; Kim et al., 2015; Strak et al., 2012; Ye et al., 2021; Yin et al., 2020).

Exposure to indoor aerosols could be more directly related to human health because people spend nearly 90% of their time indoors (Klepeis et al., 2001). Indoor biological or non-biological airborne particles can be introduced from outdoors through ventilation and infiltration (Nazaroff, 2016, 2004; Prussin and Marr, 2015), or emitted indoors through sources such as occupants, printers, and carpets (Bhangar et al., 2016; Li et al., 2020; Tian et al., 2018; Yamamoto et al., 2015; Yang et al., 2020; Yin et al., 2022). The proportion of indoor particles of outdoor origin depends on the operations and types of windows(Dai et al., 2020; Xia et al., 2021), heating, ventilation, and air conditioning (HVAC) and air filtration and disinfection systems (Feng et al., 2018b, 2021a; Wang et al., 2022), wind and temperature conditions, and building envelop permeability. Each of these factors influenced the characteristics of the particle differently within a day. For example, occupants desiring more fresh air indoors in the morning may open the windows, but in the process, facilitate the outdoor traffic-related particles ingress. Hence, the resulting diurnal trend of indoor aerosol levels is dominated by the contribution of both indoor and outdoor sources. A better understanding of the diurnal trends of indoor aerosols can help us optimize the schedule of occupancy, HVAC and air cleaning systems (Feng et al., 2021b, 2018a; Luo et al., 2022) so that it can mitigate potentially harmful aerosol exposure.

The most challenging part of experimentally investigating the diurnal trends of bioaerosols is the temporal resolution of bioaerosol sampling. Conventional culture-based methods can rely on short sampling duration (Griffiths and DeCosemo, 1994; Mainelis, 2020), but the required high intensive labor for preparing, sampling and

incubating the agar plates deter them to be used for day-and-night long-term samplings with a high temporal resolution. Besides, culture-based methods tend to be biased towards the culture medium used (Burge, 1995) and only measure culturable microorganisms (Ghosh et al., 2015; Mbareche et al., 2017) which can account for less than 1% of the total bioaerosols (Toivola et al., 2004) despite the fact that non-culturable microorganisms can be still harmful (Cox et al., 2020). Filter-based methods with DNA- or RNA- based sequencing techniques can provide abundant biological information for both viable and non-viable bioaerosols but normally require a long duration (days to weeks (Cao et al., 2014; Hospodsky et al., 2015; Kwan et al., 2020)) to collect sufficient bio-mass for DNA extraction and sequencing. In contrast, the recently emerging technique of using light-induced fluorescence (LIF) to detect bioaerosols based on their intrinsic fluorescence can provide real-time size-resolved information on both biological and non-biological airborne particles (Fennelly et al., 2017; Forde et al., 2019; Huffman et al., 2020). Though the LIF method has relatively a limited ability to differentiate between bioaerosol classes (Huffman et al., 2020), this technique can be the ideal method for evaluating the short-term dynamic of bioaerosols (Smith et al., 2022). Typical LIF-based instruments are the wideband integrated bioaerosol sensor (WIBS), the ultraviolet aerodynamic particle sizer (UV-APS), and spectral intensity bioaerosol sensor (SIBS), which are widely used for both indoor and outdoor bioaerosol measurements (Handorean et al., 2015; Ma et al., 2019; Patra et al., 2021; Pöschl et al., 2010; Tian et al., 2018; Wei et al., 2016; Yang et al., 2020).

In this study, we aim to better understand the diurnal variations of size-resolved biological and non-biological aerosols in both indoor and outdoor environments. With two units of WIBS simultaneously monitoring the indoor and outdoor aerosols for three months in a high-rise office building, we sought to evaluate the diurnal trends of a) outdoor and indoor biological and non-biological aerosols levels, b) the PM compositions in outdoor and indoor environments, and c) the outdoor and indoor relationship of biological and non-biological aerosol particles.

2 MATERIALS AND METHODS

2.1 Indoor and outdoor sampling

We conducted a continuous indoor and outdoor bioaerosol monitoring campaign from 01 October 2019 to 15 January 2020 in a typical high-rise office building (1°18'13.9"N; 103°46'24.7"E) located in the urban area in Singapore, as shown in Figure S1. The experimental site is situated near the Equator and has a typically tropical climate, with abundant rainfall, high and uniform temperatures, and high humidity all year round (Li and Tartarini, 2020; National Environment Agency, 2021). The meteorological conditions during the period of the experiment are summarized in Figure S2. The outdoor temperature was ranging from 25.7°C to 29.9 °C, and relative humidity (RH) was ranging from 68.2% to 90.1%. The daylight hours in Singapore are relatively constant around the year. During the experimental period, the sunrise was around 6:51, the sunset was around

18:55, and the solar noon was around 12:57 with a variation of ± 6 minutes, respectively. North wind, i.e., the wind blowing from land, was prevailing during the experimental period.

Two identical units of WIBS (WIBS-5/NEO, Droplet Measurement Technologies, USA) were used to simultaneously detect biological and non-biological airborne particles in both indoor and outdoor environments. The indoor and outdoor sampling locations were shown in Figure S3. The outdoor sampling was performed on the 13th floor at the outdoor air intake point of the HVAC system which served the whole building. We put the sampling instrument inside a ventilated weatherproof enclosure and used the conductive sampling tube to sample the air outside of the box. The heights of the sampling point are 1.3 m to the floor and 64 m to the ground. The horizontal distance between the outdoor sampling point to the main traffic road is around 57 m. The indoor sampling point was placed on the office desk in the middle of an open-plan office. There were 36 partitioned workstations in the office of 280 m^2 (the height from the floor to the suspended ceiling is 2.8 m). The floor of the office was fully covered by carpets (Figure S3). Most occupants are workers with a relatively flexible schedule. As shown in Figure S4, the majority of people arrived at the office before 9:00 and left around 17:30. Except for the flexible lunch break between 12:00 to 14:00, the occupancy of the office was around 12 to 15 during weekdays.

The HVAC system ventilated the office with 100% of outdoor air at a rate ranging from 1.9 to 2.1 air changes per hour (ACH). This single-pass system delivered the conditioned air into the office via terminal active chilled beams. The air was exhausted from the space with no recirculation. The HVAC system started running at 6:00 and was shut down at 20:00 every workday. During the period when the system was off, the infiltration rate ranged from 0.12 to 0.23 ACH. The air exchange rates during the mechanically ventilated and infiltration periods were quantified via the carbon dioxide (CO_2) tracer decay method detailed in a previous study(Zuraimi et al., 2022). One HOBO data logger (MX1102, HOBO®, Onset Computer Corporation, the United States) was used to monitor the indoor CO_2 temperature and RH at the indoor sampling location. As shown in Figure S2, compared with the outdoors, the indoor location had a relatively stable temperature and RH around 26.5°C and 60%, respectively. The indoor CO_2 concentration followed the occupancy, which was shown in Figure S4.

2.2 Data analysis

WIBS features as a single-particle real-time instrument for detecting bioaerosols, which provides size and fluorescent characteristics for each particle within the size range of 0.5–20 μm. The aerosol particle is first drawn through a continuous wave laser, and the resulting scattered light is detected and used to count and size all incoming particles one by one. The scatter signal sequentially triggers two Xenon flashlamps filtered to emit UV light at 280 nm and 370 nm wavelengths, respectively. Any fluorescence emitted by the particle due to these excitations is imaged onto two photomultiplier tubes equipped with filters to detect light from 310 to 400 nm and from 420 to 650 nm. With the combination of the two excitation wavelengths and two detection ranges, we can have three channels

(one channel in the combination is saturated, i.e., the excitation wavelength overlaps with the detection range.) of fluorescent information for each particle. The three channels are noted as FL1: excitation at 280 nm, emission at 310–400 nm; FL2: excitation at 280 nm, emission at 420–650 nm: and FL3: excitation at 370 nm, emission at 420–650 nm. FL1 and FL3 target the biological signature of tryptophan and nicotinamide adenine dinucleotide phosphate (NADPH) (Pöhlker et al., 2012), but FL2 does not have a clear correspondence with fluorescent biomolecules. If the fluorescence of the particle exceeds the threshold (detailed in Supporting Information) of any of the three channels, we note this particle as the fluorescent biological airborne particle (FBAP). If the particle does not reach the detection threshold of any of the three channels, it will be labeled as a non-FBAP. Further, we followed the most widely used classification method (Perring et al., 2015) to further classify FBAPs into seven subtypes noted as A, B, C, AB, AC, BC, and ABC. A, B, and C types of particles are those particles that only show fluorescence in only one of the FL1, FL2, and FL3 channels, respectively. AB, AC, and BC are those that detected the fluorescence in two of the three channels, and ABC particles are those that flagged fluorescence in all three channels. Though it is still under debate in field studies about which type is more relevant to bioaerosols (detailed in Supporting Information), this study tended to use this relatively detailed classification to reserve potentials to map the fluorescent subtypes to biological kingdoms, or even species, of bioaerosols in the future. Further, we classified the FBAPs into bacteria-like, fungi-like, and pollen-like particles according to the contributions of each fluorescent type of particles within certain thresholds of particle size ranges (Nathu et al., 2022; Nieto-Caballero, 2021; Nieto-Caballero et al., 2021), as described in Table 1.

Table 1. Classification of fluorescent particles and thresholds for defining bacteria-like, fungi-like, and pollen-like particles.

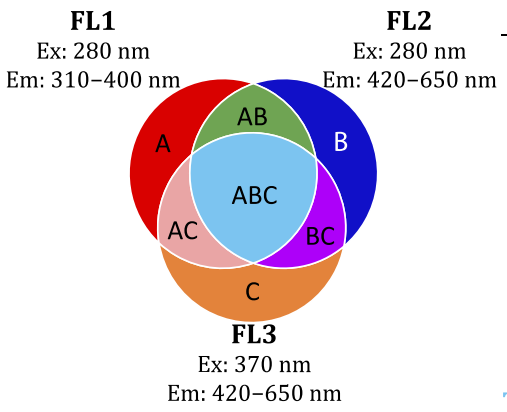

	Bacteria–like	Fungi–like	Pollen–like
Size range	0.5–1.9 μm	2.0–10 μm	1.2–10 μm
Type A contrib.	91%	80%	6%
Type B contrib.			4%
Type C contrib.			6%
Type AB contrib.	9%	15%	
Type AC contrib.			
Type BC contrib.			34%
Type ABC contrib.		5%	50%

Based on the measured diameter (D_p, μm) for each particle from the laser channel, we calculated the particle mass based on the assumed sphericity and density of 1.67 g/cm^3 (Hu et al., 2012; Pitz et al., 2008). Further, for each particle type, we aggregated particles into five size bins according to D_p: 0.5–1.0, 1.0–2.5, 2.5–5, 5–10, and 10–20 μm. The

number and mass concentrations (N_i^{type} , #/m^3 and M_i^{type} , μg/m^3) of i^{th} size bin for a certain particle type can be calculated in Eq. (1) and (2), respectively.

$$N_i^{type} = \frac{C_i^{type}}{Q \cdot T} \tag{1}$$

$$M_i^{type} = \frac{1.67 \times 10^{-6} \cdot \pi \cdot \sum_j^{C_i^{type}} \left(D_{p,j}^{type}\right)^3}{6 \cdot Q \cdot T} \tag{2}$$

where, $D_{p,j}^{type}$ is the diameter of the j^{th} particle among the total counts (C_i^{type}) in i^{th} size bin for a certain particle *type* during the sampling period (T , s). Q is the sampling flow rate in cm^3/s, and here for WIBS, Q is 5 cm^3/s. In this paper, we report the total PM, non-FBAP, FBAP, and seven subtypes of FBAP in mass concentrations that follow the unit in exposure standards for general aerosols (ASHRAE, 2016; World Health Organization, 2021) and report bacteria-like, fungi-like, and pollen-like particles in number concentrations to compare with bioaerosol studies with other methods. Besides, both number and mass concentrations of lumped and size-resolved particles in all the types are available in the Dryad repository (Li, 2022).

To better understand the indoor and outdoor relationship of aerosols, we calculated the indoor upon outdoor ratio (I/O ratio) of the mass and number concentrations according to the particle type on an hourly basis. Besides, based on mass balance modelling of aerosols, we further estimated the contributions of indoor and outdoor sources to indoor particle concentrations. For each size bin and particle type, the mass balanced model can be written as Eq. (3) or (4):

$$\frac{\mathrm{d}M_{in,i}^{type}}{\mathrm{d}t} = a_{HVAC} P_{HVAC,i}^{type} M_{out,i}^{type} + a_{shell} P_{shell,i}^{type} M_{out,i}^{type} - \left(a + k_i^{type}\right) M_{in,i}^{type} + \frac{S_{M,i}^{type}}{V} \tag{3}$$

$$\frac{\mathrm{d}N_{in,i}^{type}}{\mathrm{d}t} = a_{HVAC} P_{HVAC,i}^{type} N_{out,i}^{type} + a_{shell} P_{shell,i}^{type} N_{out,i}^{type} - \left(a + k_i^{type}\right) N_{in,i}^{type} + \frac{S_{N,i}^{type}}{V} \tag{4}$$

where, the subscripts *in* and *out* denote the indoor and outdoor environment. a_{HVAC} (1/h) and a_{shell} (1/h) are the portions of the total air exchange rate (a , 1/h) that contributed by the HVAC system and through building envelopes, respectively. $P_{HVAC,i}^{type}$

and $P_{shell,i}^{type}$ are the penetration rates of particles in i^{th} size bin through the HVAC system and the building envelope, respectively. k_i^{type} is the composite deposition rate of the *type* of particles i^{th} size bin in 1/h, which at least consist of two processes: deposition to interior surfaces and ventilation system. $S_{M,i}^{type}$ and $S_{N,i}^{type}$ are the indoor aerosol generation rate of the type of particles in i^{th} size bin in μg/h and #/s, respectively. By integrating the indoor and outdoor concentrations over a sufficient period, we can solve Eq. (3) and (4) with the steady-state assumption:

$$\overline{M_{in,i}^{type}} = \frac{\left(a_{HVAC}P_{HVAC,i}^{type} + a_{shell}P_{shell,i}^{type}\right)\overline{M_{out,i}^{type}}}{a + k_i^{type}} + \frac{S_{M,i}^{type}}{V\left(a + k_i^{type}\right)} = Inf_i^{type} \cdot \overline{M_{out,i}^{type}} + \hat{S}_{M,i}^{type} \quad (5)$$

$$\overline{N_{in,i}^{type}} = \frac{\left(a_{HVAC}P_{HVAC,i}^{type} + a_{shell}P_{shell,i}^{type}\right)\overline{N_{out,i}^{type}}}{a + k_i^{type}} + \frac{S_{N,i}^{type}}{V\left(a + k_i^{type}\right)} = Inf_i^{type} \cdot \overline{N_{out,i}^{type}} + \hat{S}_{N,i}^{type} \quad (6)$$

where, for the *type* of particle in i^{th} size bin, Inf_i^{type} (unitless) is the infiltration factor and $\hat{S}_{M,i}^{type}$ (μg/m³) and $\hat{S}_{N,i}^{type}$ (#/m³) are the source terms, which determine the contribution of outdoor and indoor sources to indoor particle concentrations, respectively. In this study, we integrated the indoor and outdoor concentrations during the HVAC was on and off for each day, respectively. Size- and type- resolved infiltration factors during the HVAC on and off can be obtained based on regression analysis, respectively. It is worth noting that, before the integration, with a similar approach as previous studies (Bi et al., 2021; Chan et al., 2018; MacNeill et al., 2012; Wu et al., 2012), we removed the data during the period with strong indoor sources to have a stronger correlation between indoors and outdoors. At last, for each type of particle, the contribution of indoor and outdoor sources ($contr.in_t^{type}$ and $contr.out^{type}$) to indoor particle concentrations can be calculated as Eq. (7) and (8).

$$
\begin{aligned}
contr.in^{type} &= \frac{\sum_{i=1}^{n} M_{in,i}^{type} - \sum_{i=1}^{n} \left(Inf_i^{type} M_{out,i}^{type} \right)}{\sum_{i=1}^{n} M_{in,i}^{type}} \times 100\% \\
contr.out^{type} &= \frac{\sum_{i=1}^{n} \left(Inf_i^{type} M_{out,i}^{type} \right)}{\sum_{i=1}^{n} M_{in,i}^{type}} \times 100\%
\end{aligned}
\tag{7}
$$

$$
\begin{aligned}
contr.in^{type} &= \frac{\sum_{i=1}^{n} N_{in,i}^{type} - \sum_{i=1}^{n} \left(Inf_i^{type} N_{out,i}^{type} \right)}{\sum_{i=1}^{n} N_{in,i}^{type}} \times 100\% \\
contr.out^{type} &= \frac{\sum_{i=1}^{n} \left(Inf_i^{type} N_{out,i}^{type} \right)}{\sum_{i=1}^{n} N_{in,i}^{type}} \times 100\%
\end{aligned}
\tag{8}
$$

2.3 Quality control

The two WIBS units were calibrated by the manufacturer annually via auto-fluorescent monodisperse polystyrene latex. We further checked the performance via a side-by-side comparison in both indoor and outdoor environments with two optical particle sizes (3330, TSI, USA). After the calibration, the results from OPS and WIBS showed relatively high consistency. As shown in Figure S5, for each size bin, the coefficient of the linear regression between the number concentrations measured by OPS and WIBS were within 0.9 to 1.1, and the values of R^2 are higher than 0.93.. To further balance out the effect of the sampling device on the indoor and outdoor relationships, we swapped the two WIBS units every week to make both units measure indoors and outdoors alternatively.

3 RESULTS AND DISCUSSION

3.1 Characteristics of outdoor airborne particles

Outdoors, there were more airborne particles during nights than days. As shown in Figure 1(a), median [interquartile range, IQR] mass concentrations of both FBAP and non-FBAP during daytime were 3.5 [3.1–4.2] μg/m^3 and 3.9 [3.3–5.2] μg/m^3, and those during nighttime were 6.7 [6.0–7.9] μg/m^3 and 5.3 [4.1–6.0] μg/m^3, which resulted in daytime and nighttime PM levels of 7.6 [6.5–9.5] μg/m^3 and 12.0 [9.7–14.0] μg/m^3, respectively. All FBAP subtypes also showed significantly higher mass concentrations during nighttime than daytime (Figure S6) with the *p*-values < 0.001 after non-parametric Mann-Whitney U tests (Table S1), among which, ABC and AC had the highest and lowest mass concentrations of 3.4 [2.6–3.5] μg/m^3 and 0.1 [0.1–0.1] μg/m^3. In Figure 1(d), bacteria-like, fungi-like, and pollen-like particles also showed higher concentrations of 119.4 [82.0–148.1] #/m^3, 1.3 [0.9–1.5] #/m^3, and 51.6 [41.0–59.6] #/m^3 during nighttime than those of 102.0 [77.8–114.3] #/m^3, 0.8 [0.6–0.9] #/m^3, and 26.3 [21.8–30.1] #/m^3 during daytime. The hourly trends of mass concentrations in Figure 1(b) indicate that PM and

FBAP levels decreased during daytime and increased during nighttime, and non-FBAP levels were relatively stable across the hours in the day. At 6:00, both FBAP and non-FBAP reached their diurnal peaks at the mass concentration of 8.2 [5.8–9.9] μg/m^3 and 5.9 [4.2–7.2] μg/m^3, respectively, which resulted in the peak value of PM at 13.8 [10.5–16.9] μg/m^3. From Figure 1(e), the concentration of pollen-like particles showed a similar trend as that of FBAP, which peaked at 6:00, whilst the levels of bacterial-like and fungi-like particles only starts decreasing after 9:00. In a previous study in Singapore (Ong, 2005), two of the three dominant types of fungal spores, *Didymosphaeria spp*. and "kuaci"(Self-named), showed a similar diurnal as this study. Even though some less prevalent species showed the opposite trend, the diurnal trend of the total amount of fungal spores in Singapore is similar to this study.

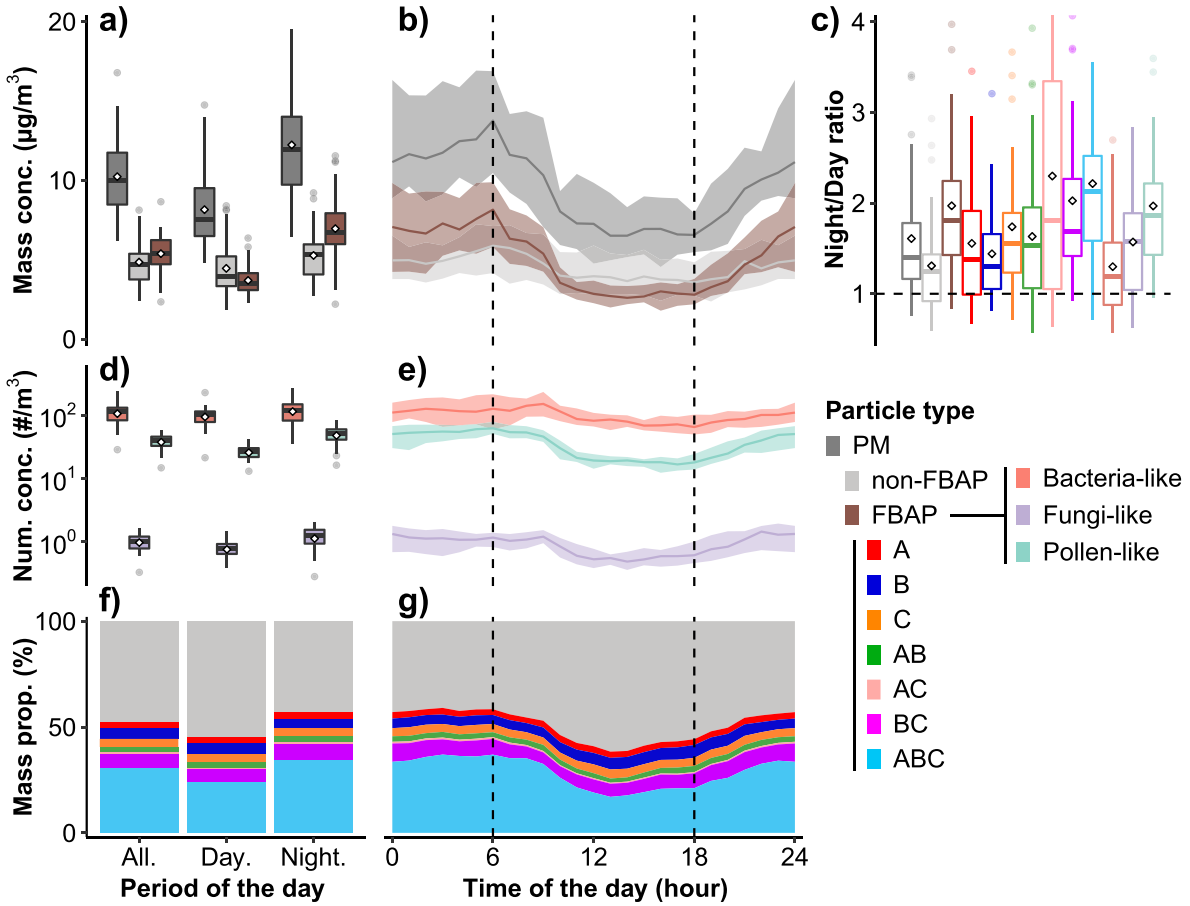

Figure 1. Diurnal trends of outdoor airborne particles within 0.5–20 μm. a) & b) mass concentrations of PM, non-FBAPs, and FBAPs, d) & e) number concentrations of bacteria-like, fungi-like, and pollen-like particles, and f) & g) PM compositions in different periods of the day and on an hourly basis, respectively. c) ratios of nighttime particle concentrations upon those of daytime for different types of particles. The boxes and ribbons in different colors are the IQR of different types of particles. Lines in the boxes and ribbons show the median value, and rhombus dots in the boxes show the mean. Whiskers of the box start from the upper and lower limits of the box and end at 1.5 times the IQR or at the maximum and minimum values if they reach first. If whiskers end at 1.5 times the IQR, the round dots are plotted as the outliers.

As shown by the daily ratio between the average concentrations during nighttime and daytime (N/D ratio) in Figure 1(c), the FBAP and non-FBAP levels at night were 1.8 [1.4–2.2] and 1.2 [0.9–1.4] times higher than those in the daytime, which resulted in the nighttime PM level was 1.4 [1.2–1.8] times higher than daytime. All FBAP subtypes also showed higher mass concentrations during nighttime than daytime, and type ABC and B had the largest and smallest diurnal variations. N/D ratios of bacteria-like, fungi-like, and pollen-like particles were 1.2 [0.9–1.6], 1.6 [1.0–1.9], and 1.9 [1.4–2.2], respectively. The characteristics of size-resolved particles are plotted in the Supporting Information. The size distributions of each particle were similar during the daytime and nighttime, as shown in Figure S7, and FBAPs and non-FBAPs were dominated by those particles in the size bins of 1–2.5 μm and 2.5–5 μm, respectively. From Figure S8, the geometric mean of the different particles outdoors was relatively stable across hours. From size-resolved results in Figure S9, for all five size ranges, N/D ratios of FBAP were always higher than those of non–FBAP: 0.5–1 μm: 1.4 [1.2–1.8] *vs.* 1.2 [1.0–1.4]; 1–2.5 μm: 1.4 [1.3–1.8] *vs.* 1.1 [0.9–1.4]; 2.5–5 μm: 1.6 [1.2–2.0] *vs.* 1.4 [0.9–1.6]; 5–10 μm: 1.9 [1.5–2.8] *vs.* 1.6 [1.1–2.0]; and 10–20 μm: 2.0 [1.3–3.6] *vs.* 1.7 [1.0–5.3]. If we sum up the first two size bins for PM concentrations from 0.5 μm to 2.5 μm, our results are similar to the previous study of global diurnal trends of $PM_{2.5}$ (Manning et al., 2018), detailed in Figure S10.

The nighttime levels of different airborne particles were higher than daytime but to different degrees, which resulted in different PM compositions during the daytime and nighttime. As shown in Figure 1(f), within the size range of 0.5–20 μm, FBAP accounted for 45% and 56% of PM during daytime and nighttime by mass, respectively. From the hourly variation of PM composition in Figure 1(g), the mass proportion of the FBAP fraction was at the lowest at 39% at 13:00 (the solar noon hour in Singapore). Then, the fraction increased to a relatively stable night value of 57%±2% from 23:00 till 6:00. After which, the FBAP fraction started to decrease again. FBAPs accounted for more than half of the aerosols from 21:00 to the next day at 9:00. From the proportions of different particles in PM in each size bin (Figure S11), the contribution of FBAPs to PM increased with the size, and FBAPs started to dominate from 2.5–5 μm. Besides, in Figure S12, the correlation coefficients between FBAP and PM are much higher than those between non-FBAP and PM, which means that FBAP could influence the dynamics of total PM concentration more than non-FBAP.

If the diurnal variation of the atmospheric mixed boundary layer thickness causes the changing of aerosol concentrations (Manning et al., 2018), it should show similar trends between non-FBAP and FBAP. However, the variation FBAP is much stronger than non-FBAP, which means other factors, such as temperature and RH that impact the different types of particles differently, need to be considered. We further examined the correlations between different aerosols and meteorological parameters from the nearest three weather stations, as shown in Figure S13. We found that the FBAP level was negatively correlated with temperature (Spearman's ρ, ρ hereafter, = -0.5) and positively correlated with RH (ρ = 0.5∼0.6), while non-FBAP did not show the correlations with temperature (ρ = -0.1) and RH (ρ = 0.1∼0.2). Within the FBAP, those correlations were dominated by

types A, AB, AC, and ABC, while types B and C did not show similar correlations. The concentrations of particles within 2.5–5 μm showed the highest correlations with temperature and RH, and smaller and larger particles were less correlated with the meteorological conditions. Hence, temperature and RH could be reasons for the diurnal variation FBAPs but not for non-FBAP.

3.2 Characteristics of indoor airborne particles

Compared to outdoors, indoors had lower airborne particle levels in general. Within the measuring range of 0.5–20 μm, mass concentrations of PM, FBAPs, and non-FBAPs were 2.8 [2.5–3.2] $\mu g/m^3$, 2.4 [2.1–2.8] $\mu g/m^3$, and 0.4 [0.2–0.5] $\mu g/m^3$, respectively, as shown in Figure 2(a). When the office was occupied, the FBAP mass concentration of 4.9 [4.2–5.5] $\mu g/m^3$ was much higher than that of 0.3 [0.2–0.4] $\mu g/m^3$ during the unoccupied period. Similarly, in Figure 2(d), bacteria-like, fungi-like, and pollen-like particles also showed a higher concentration of 48.3 [33.5–64.1] $\#/m^3$, 0.8 [0.6–0.9] $\#/m^3$, and 11.4 [9.5–13.3] $\#/m^3$ during occupied periods than those of 32.5 [21.6–47.2] $\#/m^3$, 0.1 [0.1–0.2] $\#/m^3$, and 1.5 [1.2–2.1] $\#/m^3$ during unoccupied periods. Besides the concentration, occupancy also dramatically shifted size distributions of FBAPs (Figure S7). When the room was unoccupied, the FBAPs within 2.5–5 μm dominated the indoor mass concentrations, which was similar to outdoors. However, when the room was occupied, the FBAP concentration increased monotonically along with the size. In contrast, non-FBAP showed similar concentration levels (Figure 2(a)) and monotonically decreasing size distributions (Figure S7) during both unoccupied and occupied periods. When the room was occupied, as shown in Figure 2(f), FBAPs accounted for 87% of PM, while when it was unoccupied, the indoor FBAP proportion in PM was 47% which is similar to the percentage outdoors.

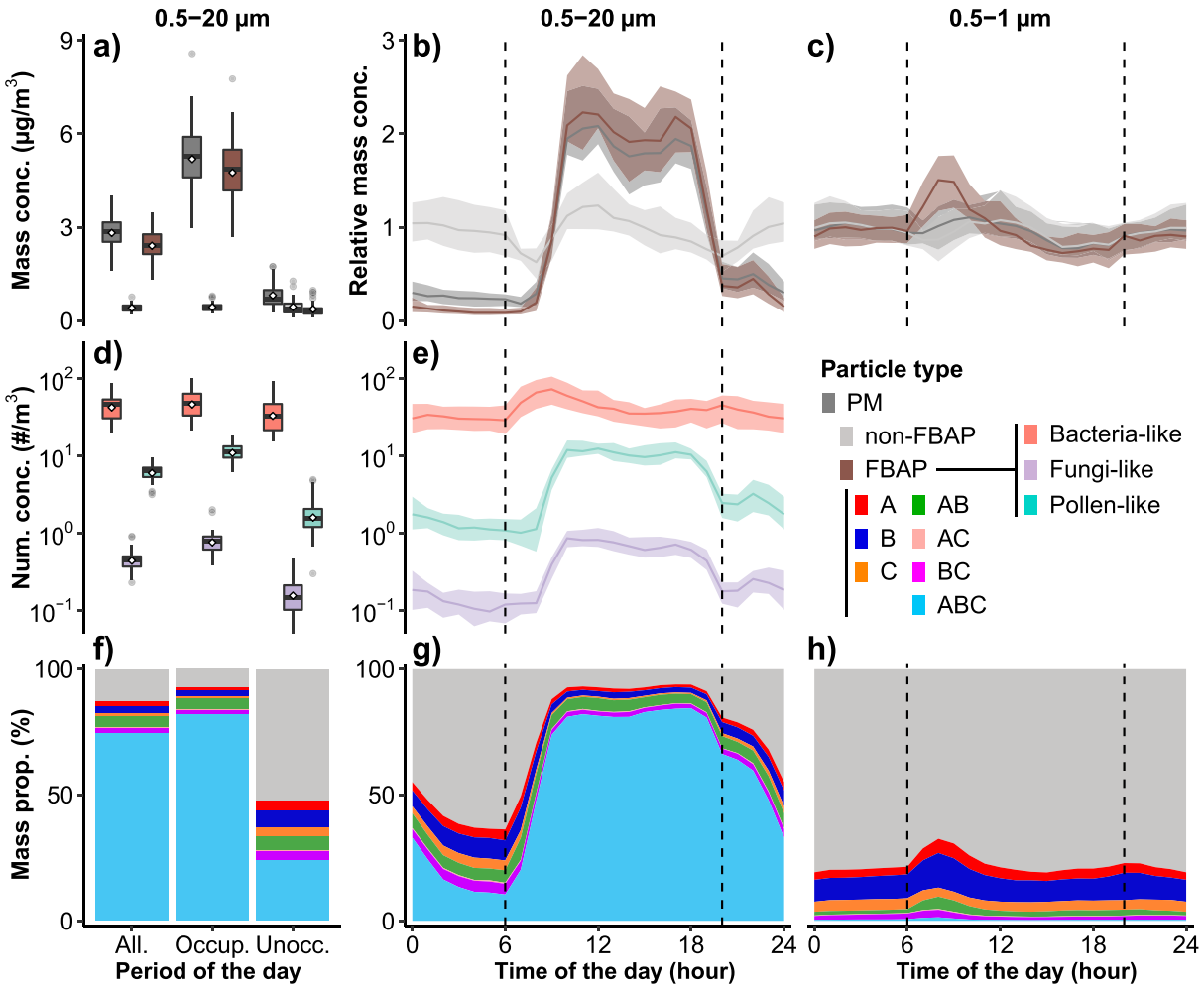

Figure 2. Diurnal trends of indoor airborne particles. a) mass concentrations & b) relative mass concentrations of PM, non-FBAPs, and FBAPs, d) & e) number concentrations of bacteria-like, fungi-like, and pollen-like particles, and f) & g) PM compositions within 0.5–20 μm in different periods or at different times of the day. c) relative mass concentration of PM, non-FBAPs, and FBAPs and h) PM compositions within 0.5–1 μm at different times of the day.

The lumped level of indoor FBAPs within 0.5–20 μm was driven by the variation of occupancy levels. From the relative mass concentration which was normalized by the daily average concentration for each particle type in Figure 2(b), the indoor mass concentration of FBAPs shot up at 9:00 when people arrived and remained at a relatively stable level till 18:00 when people started to gradually leave the room. From the size-resolved normalized particle concentrations in Figure S14, except the smallest one of 0.5–1 μm (to be detailed separately later), all other size ranges (2.5–5 μm, 5–10 μm, and 10–20 μm) showed similar trends as the integrated one in Figure 2(b). The trends of fungi-like and pollen-like particles with larger sizes are similar to that of FBAPs, as shown in Figure 2(e). In contrast, the non-FBAPs showed a much milder increase when occupants arrived than FBAPs, which caused FBAPs to dominate PM during the occupied period. These inconsistent variations of FBAPs and non-FBAPs caused large changes in the PM compositions throughout the day. In Figure 2(g), the lowest and the highest FBAP proportions were 34% in PM at 6:00 and 94% at 17:00. The correlations between

different particle levels and indoor levels of temperature, RH, and CO_2 were shown in Figure S15. The CO_2 concentration, as an indicator of occupancy, showed positive correlations with the total concentrations of all types of particles ($\rho = 0.5 \sim 0.7$), and the occupancy showed the similar positive correlations but with lower coefficients. This further supported our hypothesis that the occupancy levels strongly influenced the indoor particle level.

We next observed a situation where indoor FBAP levels, in particular the smallest size bin (0.5–1 μm) and bacteria-like particles, increased before the occupants arrived. The increase in concentrations started at 6:00 when the HVAC system began to operate. As shown in Figure 2(c), the levels peaked at 8:00 where the normalized concentration is 1.5 [1.2–1.8]. The FBAP concentration in this size bin only reduced down to the daily average at noontime. Concurrently, the proportion of FBAPs in PM in this size bin peaked at 8:00 and reduced down to the daily average at noon. In the second size bin (1–2.5 μm) shown in Figure S14, though we didn't see a similar increase of FBAPs after the HVAC system started running, the sudden decrease of non-FBAPs caused the proportion of the FBAP proportion in PM also peaked at 8:00. Similarly, the concentration of bacteria-like particles in Figure 2(e) increased after the operation of the HVAC system and peaked at 9:00 with a concentration of 73.2 [46.3–107.1] #/m^3. These indicated that the HVAC system of the building was a temporary source of indoor fine FBAPs when it started running. We speculated that, after the HVAC system was turned off at 20:00, the ductwork and coils became reservoirs for bioaerosols to multiply overnight (Acerbi et al., 2017; Wu et al., 2016; Zuraimi, 2010; Zuraimi et al., 2012). When the system began operating the following morning, the mechanical vibration and airflow dislodged the settled aerosols into the indoor environment. Due to the fact that outdoor air was treated with MERV13 filters, most of the larger FBAPs, like fungi and pollens, were prevented from entering the HVAC system and accumulating in ductwork and on coils. Indeed, we didn't observe any spikes in coarse FBAPs concentration levels when the HVAC system started running. Elsewhere, a Hong Kong study also observed the peak of bioaerosols when the HVAC system started running (Law et al., 2001).

3.3 Indoor and outdoor relationships of airborne particles

In Figure 3(a), FBAPs showed a much higher indoor upon outdoor (I/O) ratio of 0.46 [0.40–0.66] than non-FBAPs 0.09 [0.08–0.11] throughout the day, which resulted in the ratio of 0.31 [0.24–0.38] for PM. However, the indoor and outdoor relationships greatly varied in different periods of the day. During the unoccupied period, the I/O ratios of FBAPs and non-FBAPs were similar (0.06 [0.04–0.07] vs. 0.07 [0.06–0.10]). In contrast, when the room was occupied, the I/O ratio of FBAP showed a much higher I/O ratio of 1.54 [1.16–1.77], which drove the ratio of PM to reach 0.81 [0.59–0.94], but that of non-FBAP showed a much milder increase compared with unoccupied periods. Bacteria-like, fungi-like, and pollen-like particles also showed a higher I/O ratio during the occupied period, as shown in Figure 3(c), and pollen-like particles had the lowest I/O ratio among the three.

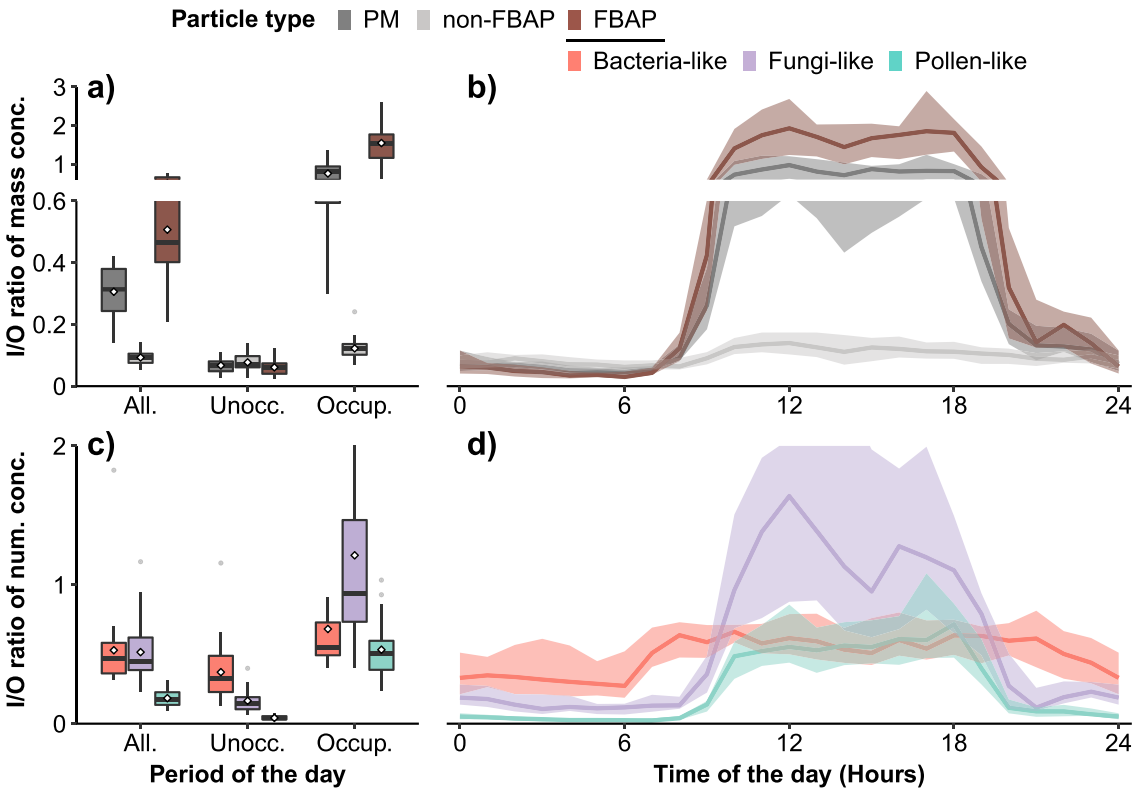

Figure 3. Indoor and outdoor relationship of a) & b) PM, non-FBAPs, and FBAPs and c) & d) bacteria-like, fungi-like, and pollen-like particles in different periods and at different times of the day.

The diurnal trends of the I/O ratio of PM and FBAPs were dominated by those of indoor concentrations. From the diurnal trends in Figure 3(b), I/O ratios PM and FBAPs dramatically increased when people arrived at the office around 9:00 and kept at relatively stable levels until 18:00 when most people left the office. In Figure 3(d), I/O ratios of fungi-like and pollen-like particles showed a similar trend with FBAP, whilst that of bacteria-like particles increased when the HVAC started operation. The fungi-like and pollen-like particles showed interesting but counterintuitive associations with occupancy. It means that, in the office building with a relatively high-efficiency air filtration system, fungi and pollen may hardly enter the space from outdoors but be brought in by people. Especially for fungi-like particles with the highest I/O ratio during the occupied period, a large amount of those particles in indoor air be sourced from human-induced resuspension from the carpet which serves as a reservoir of fungi (Dannemiller et al., 2017; Haines et al., 2020; Lewis et al., 2018; Wu et al., 2018).

Among FBAP subtypes shown in Figure S16, type ABC and AB had much higher I/O ratios during the occupied periods than those of other types, while type C showed the lowest I/O ratio of the particle concentration. The I/O ratio of size-resolved particle concentrations were shown in Figure S17. During the unoccupied period for all types of particles, the I/O ratios decayed monotonically with the increase of particle sizes because larger particles are harder to penetrate indoors (Chen and Zhao, 2011). However, during the occupied period, the I/O ratio showed an increasing trend along with the particle size, which indicated that indoors generated larger particles. This indicated that occupancy, or

occupant-related activity, generated much more FBAP than non-FBAP and larger particles than smaller ones, which was aligned with quantified per-person emission rates of different types of particles in the previous chamber and field studies (Li et al., 2020; Tian et al., 2018; Yang et al., 2020; Zhou et al., 2017).

Based on the estimated two infiltration factors when the HVAC was on and off for each type of particle (Figure S18), we summarized contributions of indoor and outdoor aerosols to indoor particle concentration on an hourly basis in Figure 4. During most times of the day, the indoor environment contributed more aerosols to indoor sources than outdoors. Especially during the occupied period, the indoor contributions of PM, non-FBAPs, FBAPs, bacteria-like particles, fungi-like particles, and pollen-like particles to indoors were 93%, 67%, 97%, 61%, 97%, and 95% on average, respectively. After the HVAC system shut down at 20:00, the office was partially occupied with few people working overtime, and the contributions of indoor sources started to increase until the room was fully empty around 23:00. Especially for bacteria-like particles, the indoor contribution reached 83.3% which was the highest throughout the day. From midnight, the contribution of outdoor sources started to increase until the morning the next day when the room was occupied again. During the unoccupied period, the contributions of indoor sources of PM, non-FBAPs, and FBAPs decreased to a very similar level around 54%. From size-resolved indoor and outdoor contributions of indoor aerosols in Figure S19, the indoor contributions of indoor aerosols increased with the particle size during the occupied period, and for particles larger than 5 μm, nearly all the FBAPs were from indoor sources. In contrast, during the unoccupied period, the contributions of different sources to indoor aerosols were similar across size ranges. It is worth noting that the estimated contributions of different sources only based on indoor and outdoor concentrations can give us a coarse estimation during the day but cannot provide a detailed classification of the real origin of the particle. For example, the increase and indoor concentrations of FBAPs when the HVAC systems started running did not associate with a concurrent increase of outdoor concentration, so the contribution of that increase was classified as indoor.

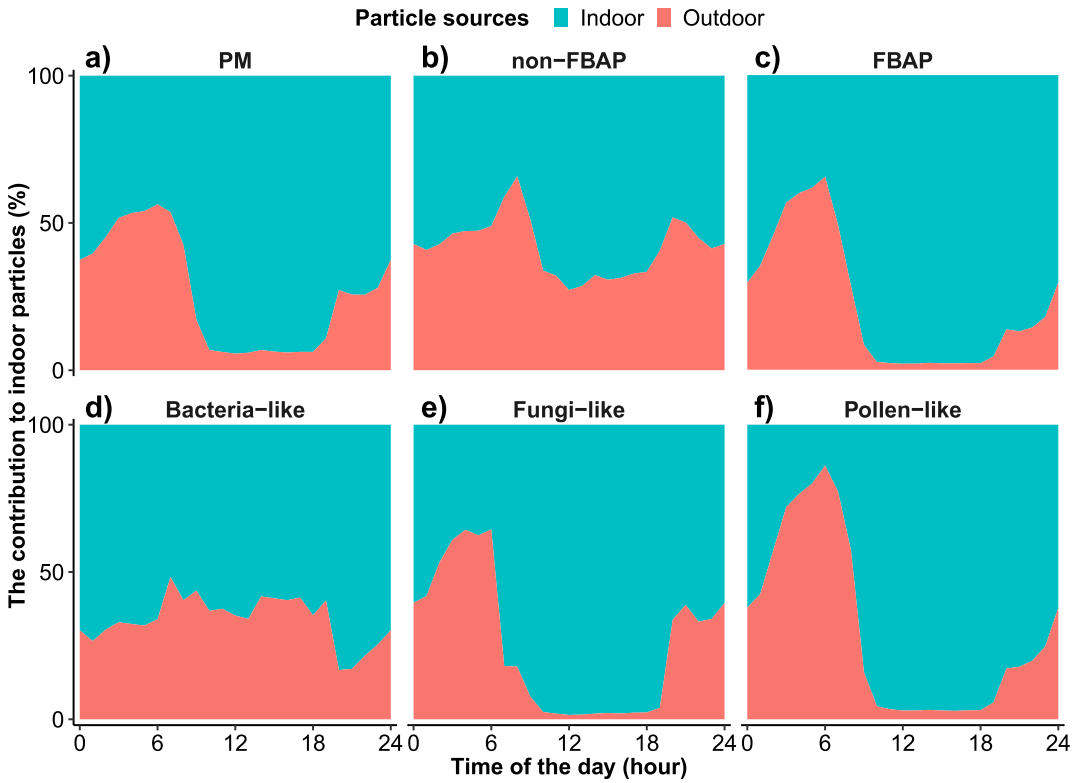

Figure 4. Diurnal variations of the contribution of indoor and outdoor sources to indoor aerosols for a) PM, b) non-FABP, c) FABP, d) bacterial-like, e) fungi-like and f) pollen-like particles.

3.4 Limitations

This study has several limitations. First, though WIBS provides size-resolved dynamic results of aerosols with a high temporal resolution, we still currently lack sufficient understanding of the relationship between the measured FBAPs and bioaerosols. Recently researchers have tried various strategies to map the fluorescent signals from three channels with different species; more details are given in the Supporting Information. Though those studies showed the potential of mapping different FBAPs to different microorganism species in a chamber study (Hernandez et al., 2016), there is still a lack of a consensus on the understanding of FBAPs in the field measurement. In the chamber study, the separately released species showed differentiable fluorescent signals among each other, whilst different types of particles may coagulate together in fields. If a non-FBAP and a FBAP coagulated together, WIBS will tend to report it as FBAP. If three particles in types A, B, and C coagulated together or attached to form one large particle, the instrument will flag it as a Type ABC particle. To retain the potential of further understanding FBAPs, we will upload all the measured raw data in the Dryad database (Li, 2022).

Secondly, this study has the limitation of a single sampling site. Though the patterns of bioaerosols at different sampling locations in the tropics were similar (Gusareva et al., 2019), those findings may not be directly applicable to other climates or areas with high anthropogenic emissions. Besides, indoor diurnal trends may vary based on the function

of the building, the ventilation type, and occupancy. The diurnal trend of indoor particle levels in this study only can be representative of similar types of office buildings.

Third, the regression-based indoor and outdoor aerosol modeling to estimate the contributions of different sources was limited by the steady-state assumption. As an example, we can see a constantly decreasing indoor aerosol level during the nighttime, which means the steady state has not been fully reached. However, we mitigate this by using the averaged aerosol concentrations during two relatively long periods when the HVAC on and off in the regression model. Besides, similar to the study (Wu et al., 2012), we used the regression method to model the indoor and outdoor particle relationship, the low R^2 in the regressions for coarse particles limited the accuracy of the estimation.

3.5 Implications and future outlook

Human exposure to bioaerosols is related to the risk of infection and allergy. Diurnal trend information on indoor and outdoor levels of bioaerosols can guide people, especially the susceptible ones, to avoid the relatively high-level periods so that they can lower their daily bioaerosols exposure. The outdoor trends of FBAPs indicated that people could mitigate bioaerosols exposure by reducing outdoor time at night. For example, we would suggest people shift some nighttime outdoor exercises to the daytime when possible. Naturally ventilated buildings, that usually do not have a filtration system, should have open windows after 9:00 to reduce the exposure to outdoor bioaerosols, unfortunately this is also the time with the highest outdoor temperatures and therefore not convenient in tropical climates. However, we don't have much information about the exposure risks of FBAPs regarding health impact, which need to study further.

Those indoor diurnal trends also can be used to design intervention strategies to lower bioaerosol exposure in commercial buildings. We could consider shifting the turning on of the HVAC fan earlier to avoid occupants exposing to the morning peak of fine bioaerosols or redesign the HVAC with the function of expelling the overnight accumulated bioaerosols outdoors before sending the air indoors. The indoor and outdoor relationships revealed that the bioaerosols were more from indoors than outdoors for this type of office buildings with a high-efficiency filtration system in the HVAC system. The HVAC successfully reduced the contributions of outdoor sources to indoors but didn't control the indoor sources well. Compared to this dilution-based centralized method of ventilation for controlling indoor sources, we could further consider adding localized solutions, such as portable air cleaners or local exhaust, which are targeted to those indoor sources to further lowering down the indoor aerosol levels.

4 CONCLUSIONS

In this study, with the real-time instruments for measuring size-resolved bioaerosols, we provided diurnal trends and relationships of indoor and outdoor FBAPs and non-FBAPs, which not only contribute to the understanding of bioaerosol dynamics in the tropics but also provide instructive meaning for lowering bioaerosol exposure. The main findings are summarized as follows:

1. Outdoors, there were more airborne particles during nights than days. Nighttime concentrations of FBAP and non-FBAP were 6.7 [6.0–7.9] μg/m^3 and 5.3 [4.1–6.0] μg/m^3, which were 1.8 [1.4–2.2] and 1.2 [0.9–1.4] higher than those of 3.5 [3.1–4.2] μg/m^3 and 3.9 [3.3–5.2] μg/m^3 during the daytime, respectively.
2. Outdoor FBAP concentrations decreased during daytime and increased during nighttime, and non-FBAP concentrations were relatively stable across the hours in the day. At 6:00, FBAP reached their diurnal peaks at the mass concentration of 8.2 [5.8–9.9] μg/m^3. FBAP accounted for 45% and 56% of PM during daytime and nighttime by mass, respectively. The proportion of the FBAP fraction in PM was at the lowest at 39% at 13:00 around the local solar noon hour.
3. Indoors, the lumped mass concentration of FBAPs within 0.5–20 μm was highly associated with occupancy. When the office was occupied, the indoor FBAP mass concentration of 4.9 [4.2–5.5] μg/m^3 was much higher than that of 0.3 [0.2–0.4] μg/m^3 during the unoccupied period.
4. The HVAC system of the building was a temporary source of indoor fine FBAPs when it started running. The concentrations of indoor fine FBAPs and bacteria-like particles increased when the HVAC started operating around 6:00 and peaked around 8:00.
5. Indoor airborne particles were more contributed by indoor sources than outdoor sources. Based on regression modeling, the contributions of indoor PM, non-FBAP, FBAP, bacteria-like particle, fungi-like particle, and pollen-like particle sources to indoor mass concentrations were estimated to be 93%, 67%, 97%, 61%, 97%, and 95% during the occupied period.

5 SUPPORTING INFORMATION

Supporting information and additional figures and tables as described in the text can be found can be found online at https://doi.org/10.1016/j.scitotenv.2022.157811, which includes:

Figure S1. The building (CREATE Tower) for the indoor and outdoor bioaerosol sampling and its location in Singapore. The image of building is from www.dpa.com.sg/projects/createatnus/. The location map is from Google Maps.

Figure S2. Meteorological conditions. The outdoor temperature and relative humidity were based on the nearest three available stations: S50 (1.3337, 103.7768), S116 (1.281, 103.754), and S111 (1.31055, 103.8365), and the wind rose was based on the nearest available station S50. The indoor temperature and RH were measured by HOBO CO_2 MX1102 on the office desk.

Figure S3. Indoor and outdoor sampling location of wideband integrated bioaerosol sensors (WIBSs).

Figure S4. Summary of the indoor CO_2 concentration and occupancy profiles of the experimental days (weekdays).

Figure S5. Linear regressions between the number concentrations measured by the WIBS and OPS.

Figure S6. Mass concentrations of different types of particles within 0.5-20 μm.

Figure S7. Size-resolved mass concentrations of different types of particles.

Figure S8. The diurnal trend of the size of aerosols.

Figure S9. Size-resolved mass concentrations and the ratio of the concentrations during nighttime upon daytime in outdoors

Figure S10. The comparison between the global diurnal trend of PM2.5 (Manning et al., 2018) and the PM within 0.5 to 2.5 μm.

Figure S11. Size-resolved indoor and outdoor PM compositions during different periods of the day.

Figure S12. Spearman's rank-order correlations between mass/number concentrations of all the particle types in outdoor and indoor environments.

Figure S13. Correlations between outdoor mass concentrations of all size ranges and particle types and meteorological conditions.

Figure S14. Diurnal trends of indoor airborne particles within the size ranges of 1–2.5, 2.5–5, 5–10, and 10–20 μm.

Figure S15. Correlations between indoor mass concentrations of all size ranges and particle types and indoor temperature, RH, and CO_2.

Figure S16. Indoor and outdoor relationship of subtypes of FBAPs

Figure S17. Size-resolved I/O ratios of all types of aerosols.

Figure S18. Size-resolved infiltration factors for PM, non-FBAPs, and FBAPs.

Figure S19. Size-resolved contributions of indoor and outdoor sources to indoor particle concentrations.

Table S1. The outdoor mass concentrations of PM, non-FBAP, FBAP, A, B, C, AB, AC, BC, and ABC particles and the significant levels of the difference between those in the daytime and nighttime.

Table S2. The outdoor number concentrations of bacteria-like, fungi-like, and pollen-like particles and the significant levels of the differences between those in the daytime and nighttime.

Table S3. The indoor mass concentrations of PM, non-FBAP, FBAP, A, B, C, AB, AC, BC, and ABC particles and the significant levels of the difference between those in the daytime and nighttime.

Table S4. The indoor number concentrations of bacteria-like, fungi-like, and pollen-like particles and the significant levels of the differences between those in the daytime and nighttime.

6 ACKNOWLEDGMENT

This research was funded by the Republic of Singapore's National Research Foundation through a grant to the Berkeley Education Alliance for Research in Singapore (BEARS) for the Singapore-Berkeley Building Efficiency and Sustainability in the Tropics (SinBerBEST) Program. BEARS has been established by the University of California, Berkeley as a center for intellectual excellence in research and education in Singapore.

7 REFERENCES

Acerbi, E., Chénard, C., Miller, D., Gaultier, N.E., Heinle, C.E., Chang, V.W.-C., Uchida, A., Drautz-Moses, D.I., Schuster, S.C., Lauro, F.M., 2017. Ecological succession of the microbial communities of an air-conditioning cooling coil in the tropics. Indoor Air 27, 345–353. https://doi.org/10.1111/ina.12306

ASHRAE, 2016. Standard 62.1: Ventilation for Acceptable Indoor Air Quality. ASHRAE.

Bhangar, S., Adams, R.I., Pasut, W., Huffman, J.A., Arens, E.A., Taylor, J.W., Bruns, T.D., Nazaroff, W.W., 2016. Chamber bioaerosol study: human emissions of size-resolved fluorescent biological aerosol particles. Indoor Air 26, 193–206. https://doi.org/10.1111/ina.12195

Bi, J., Wallace, L.A., Sarnat, J.A., Liu, Y., 2021. Characterizing outdoor infiltration and indoor contribution of PM2.5 with citizen-based low-cost monitoring data. Environ. Pollut. 276, 116763. https://doi.org/10.1016/j.envpol.2021.116763

Burge, H.A., 1995. Bioaerosols. CRC Press.

Cao, C., Jiang, W., Wang, B., Fang, J., Lang, J., Tian, G., Jiang, J., Zhu, T.F., 2014. Inhalable Microorganisms in Beijing's PM2.5 and PM10 Pollutants during a Severe Smog Event. Environ. Sci. Technol. 48, 1499–1507. https://doi.org/10.1021/es4048472

Chan, W.R., Logue, J.M., Wu, X., Klepeis, N.E., Fisk, W.J., Noris, F., Singer, B.C., 2018. Quantifying fine particle emission events from time-resolved measurements: Method description and application to 18 California low-income apartments. Indoor Air 28, 89–101. https://doi.org/10.1111/ina.12425

Chen, C., Zhao, B., 2011. Review of relationship between indoor and outdoor particles: I/O ratio, infiltration factor and penetration factor. Atmos. Environ. 45, 275–288. https://doi.org/10.1016/j.atmosenv.2010.09.048

Cox, J., Mbareche, H., Lindsley, W.G., Duchaine, C., 2020. Field sampling of indoor bioaerosols. Aerosol Sci. Technol. 54, 572–584. https://doi.org/10.1080/02786826.2019.1688759

Dai, X., Liu, J., Zhang, X., 2020. A review of studies applying machine learning models to predict occupancy and window-opening behaviours in smart buildings. Energy Build. 223, 110159. https://doi.org/10.1016/j.enbuild.2020.110159

Dannemiller, K.C., Weschler, C.J., Peccia, J., 2017. Fungal and bacterial growth in floor dust at elevated relative humidity levels. Indoor Air 27, 354–363. https://doi.org/10.1111/ina.12313

Després, VivianeR., Huffman, J.A., Burrows, S.M., Hoose, C., Safatov, AleksandrS., Buryak, G., Fröhlich-Nowoisky, J., Elbert, W., Andreae, MeinratO., Pöschl, U., Jaenicke, R., 2012. Primary biological aerosol particles in the atmosphere: a review. Tellus B Chem. Phys. Meteorol. 64, 15598. https://doi.org/10.3402/tellusb.v64i0.15598

Feng, Z., Cao, S.-J., Haghighat, F., 2021a. Removal of SARS-CoV-2 using UV+Filter in built environment. Sustain. Cities Soc. 74, 103226. https://doi.org/10.1016/j.scs.2021.103226

Feng, Z., Cao, S.-J., Wang, J., Kumar, P., Haghighat, F., 2021b. Indoor airborne disinfection with electrostatic disinfector (ESD): Numerical simulations of ESD performance and reduction of computing time. Build. Environ. 107956. https://doi.org/10.1016/j.buildenv.2021.107956

Feng, Z., Long, Z., Adamiak, K., 2018a. Numerical simulation of electrohydrodynamic flow and vortex analysis in electrostatic precipitators. IEEE Trans. Dielectr. Electr. Insul. 25, 404–412. https://doi.org/10.1109/TDEI.2017.006550

Feng, Z., Pan, W., Wang, Y., Long, Z., 2018b. Modeling filtration performance of pleated fibrous filters by Eulerian-Markov method. Powder Technol. 340, 502–510. https://doi.org/10.1016/j.powtec.2018.09.037

Fennelly, M., Sewell, G., Prentice, M., O'Connor, D., Sodeau, J., Fennelly, M.J., Sewell, G., Prentice, M.B., O'Connor, D.J., Sodeau, J.R., 2017. The use of real-time fluorescence instrumentation to monitor ambient primary biological aerosol particles (PBAP). Atmosphere 9, 1. https://doi.org/10.3390/atmos9010001

Forde, E., Gallagher, M., Walker, M., Foot, V., Attwood, A., Granger, G., Sarda-Estève, R., Stanley, W., Kaye, P., Topping, D., 2019. Intercomparison of Multiple UV-LIF Spectrometers Using the Aerosol Challenge Simulator. Atmosphere 10, 797. https://doi.org/10.3390/atmos10120797

Ghosh, B., Lal, H., Srivastava, A., 2015. Review of bioaerosols in indoor environment with special reference to sampling, analysis and control mechanisms. Environ. Int. 85, 254–272. https://doi.org/10.1016/j.envint.2015.09.018

Griffiths, W.D., DeCosemo, G.A.L., 1994. The assessment of bioaerosols: A critical review. J. Aerosol Sci. 25, 1425–1458. https://doi.org/10.1016/0021-8502(94)90218-6

Gusareva, E.S., Acerbi, E., Lau, K.J.X., Luhung, I., Premkrishnan, B.N.V., Kolundžija, S., Purbojati, R.W., Wong, A., Houghton, J.N.I., Miller, D., Gaultier, N.E., Heinle, C.E., Clare, M.E., Vettath, V.K., Kee, C., Lim, S.B.Y., Chénard, C., Phung, W.J., Kushwaha, K.K., Nee, A.P., Putra, A., Panicker, D., Yanqing, K., Hwee, Y.Z., Lohar, S.R., Kuwata, M., Kim, H.L., Yang, L., Uchida, A., Drautz-Moses, D.I., Junqueira, A.C.M., Schuster, S.C., 2019. Microbial communities in the tropical air ecosystem follow a precise diel cycle. Proc. Natl. Acad. Sci. 116, 23299–23308. https://doi.org/10.1073/pnas.1908493116

Haines, S.R., Adams, R.I., Boor, B.E., Bruton, T.A., Downey, J., Ferro, A.R., Gall, E., Green, B.J., Hegarty, B., Horner, E., Jacobs, D.E., Lemieux, P., Misztal, P.K., Morrison, G., Perzanowski, M., Reponen, T., Rush, R.E., Virgo, T., Alkhayri, C., Bope, A., Cochran, S., Cox, J., Donohue, A., May, A.A., Nastasi, N., Nishioka, M., Renninger, N., Tian, Y., Uebel-Niemeier, C., Wilkinson, D., Wu, T., Zambrana, J., Dannemiller, K.C., 2020. Ten questions concerning the implications of carpet on indoor chemistry and microbiology. Build. Environ. 170, 106589. https://doi.org/10.1016/j.buildenv.2019.106589

Handorean, A., Robertson, C.E., Harris, J.K., Frank, D., Hull, N., Kotter, C., Stevens, M.J., Baumgardner, D., Pace, N.R., Hernandez, M., 2015. Microbial aerosol liberation from soiled textiles isolated during routine residuals handling in a modern health care setting. Microbiome 3, 72. https://doi.org/10.1186/s40168-015-0132-3

Harrison, R.M., Yin, J., 2000. Particulate matter in the atmosphere: which particle properties are important for its effects on health? Sci. Total Environ. 249, 85–101. https://doi.org/10.1016/S0048-9697(99)00513-6

Hernandez, M., Perring, A.E., McCabe, K., Kok, G., Granger, G., Baumgardner, D., 2016. Chamber catalogues of optical and fluorescent signatures distinguish bioaerosol classes. Atmospheric Meas. Tech. 9, 3283–3292. https://doi.org/10.5194/amt-9-3283-2016

Hospodsky, D., Yamamoto, N., Nazaroff, W.W., Miller, D., Gorthala, S., Peccia, J., 2015. Characterizing airborne fungal and bacterial concentrations and emission rates in six occupied children's classrooms. Indoor Air 25, 641–652. https://doi.org/10.1111/ina.12172

Hu, M., Peng, J., Sun, K., Yue, D., Guo, S., Wiedensohler, A., Wu, Z., 2012. Estimation of size-resolved ambient particle density based on the measurement of aerosol number, mass, and chemical size distributions in the winter in Beijing. Environ. Sci. Technol. 46, 9941–9947. https://doi.org/10.1021/es204073t

Huang, S., Hu, W., Chen, J., Wu, Z., Zhang, D., Fu, P., 2021. Overview of biological ice nucleating particles in the atmosphere. Environ. Int. 146, 106197. https://doi.org/10.1016/j.envint.2020.106197

Huffman, J.A., Perring, A.E., Savage, N.J., Clot, B., Crouzy, B., Tummon, F., Shoshanim, O., Damit, B., Schneider, J., Sivaprakasam, V., Zawadowicz, M.A., Crawford, I., Gallagher, M., Topping, D., Doughty, D.C., Hill, S.C., Pan, Y., 2020. Real-time sensing of bioaerosols: Review and current perspectives. Aerosol Sci. Technol. 54, 465–495. https://doi.org/10.1080/02786826.2019.1664724

Jaenicke, R., 2005. Abundance of Cellular Material and Proteins in the Atmosphere. Science 308, 73–73. https://doi.org/10.1126/science.1106335

Kelly, F.J., Fussell, J.C., 2012. Size, source and chemical composition as determinants of toxicity attributable to ambient particulate matter. Atmos. Environ. 60, 504–526. https://doi.org/10.1016/j.atmosenv.2012.06.039

Kim, K.-H., Kabir, E., Jahan, S.A., 2018. Airborne bioaerosols and their impact on human health. J. Environ. Sci. 67, 23–35. https://doi.org/10.1016/j.jes.2017.08.027

Kim, K.-H., Kabir, E., Kabir, S., 2015. A review on the human health impact of airborne particulate matter. Environ. Int. 74, 136–143. https://doi.org/10.1016/j.envint.2014.10.005

Klepeis, N.E., Nelson, W.C., Ott, W.R., Robinson, J.P., Tsang, A.M., Switzer, P., Behar, J.V., Hern, S.C., Engelmann, W.H., 2001. The National Human Activity Pattern Survey (NHAPS): a resource for assessing exposure to environmental pollutants. J. Expo. Anal. Environ. Epidemiol. 11, 231–52.

Kwan, S.E., Shaughnessy, R., Haverinen-Shaughnessy, U., Kwan, T.A., Peccia, J., 2020. The Impact of Ventilation Rate on the Fungal and Bacterial Ecology of Home Indoor Air. Build. Environ. 106800. https://doi.org/10.1016/j.buildenv.2020.106800

Law, A.K.Y., Chau, C.K., Chan, G.Y.S., 2001. Characteristics of bioaerosol profile in office buildings in Hong Kong. Build. Environ. 36, 527–541. https://doi.org/10.1016/S0360-1323(00)00020-2

Lewis, R.D., Ong, K.H., Emo, B., Kennedy, J., Kesavan, J., Elliot, M., 2018. Resuspension of house dust and allergens during walking and vacuum cleaning. J. Occup. Environ. Hyg. 15, 235–245. https://doi.org/10.1080/15459624.2017.1415438

Li, J., 2022. Data from: Diurnal trends of indoor and outdoor fluorescent biological aerosol particles in a tropical urban area. Dryad Dataset. https://doi.org/10.6078/D1WD9W

Li, J., Tartarini, F., 2020. Changes in Air Quality during the COVID-19 Lockdown in Singapore and Associations with Human Mobility Trends. Aerosol Air Qual. Res. 20, 1748–1758. https://doi.org/10.4209/aaqr.2020.06.0303

Li, J., Wan, M.P., Schiavon, S., Tham, K.W., Zuraimi, S., Xiong, J., Fang, M., Gall, E., 2020. Size-resolved dynamics of indoor and outdoor fluorescent biological aerosol particles in

a bedroom: A one-month case study in Singapore. Indoor Air 30, 942–954. https://doi.org/10.1111/ina.12678

Luo, Y., Cheng, N., Zhang, S., Tian, Z., Xu, G., Yang, X., Fan, J., 2022. Comprehensive energy, economic, environmental assessment of a building integrated photovoltaic-thermoelectric system with battery storage for net zero energy building. Build. Simul. https://doi.org/10.1007/s12273-022-0904-1

Ma, Y., Wang, Z., Yang, D., Diao, Y., Wang, W., Zhang, H., Zhu, W., Zheng, J., 2019. On-line measurement of fluorescent aerosols near an industrial zone in the Yangtze River Delta region using a wideband integrated bioaerosol spectrometer. Sci. Total Environ. 656, 447–457. https://doi.org/10.1016/j.scitotenv.2018.11.370

MacNeill, M., Wallace, L., Kearney, J., Allen, R.W., Van Ryswyk, K., Judek, S., Xu, X., Wheeler, A., 2012. Factors influencing variability in the infiltration of PM2.5 mass and its components. Atmos. Environ. 61, 518–532. https://doi.org/10.1016/j.atmosenv.2012.07.005

Mainelis, G., 2020. Bioaerosol sampling: Classical approaches, advances, and perspectives. Aerosol Sci. Technol. 54, 496–519. https://doi.org/10.1080/02786826.2019.1671950

Manning, M.I., Martin, R.V., Hasenkopf, C., Flasher, J., Li, C., 2018. Diurnal patterns in global fine particulate matter concentration. Environ. Sci. Technol. Lett. 5, 687–691.

Marcovecchio, F., Perrino, C., 2021. Contribution of Primary Biological Aerosol Particles to airborne particulate matter in indoor and outdoor environments. Chemosphere 264, 128510. https://doi.org/10.1016/j.chemosphere.2020.128510

Mbareche, H., Brisebois, E., Veillette, M., Duchaine, C., 2017. Bioaerosol sampling and detection methods based on molecular approaches: No pain no gain. Sci. Total Environ. 599–600, 2095–2104. https://doi.org/10.1016/j.scitotenv.2017.05.076

Morawska, L., Ayoko, G.A., Bae, G.N., Buonanno, G., Chao, C.Y.H., Clifford, S., Fu, S.C., Hänninen, O., He, C., Isaxon, C., Mazaheri, M., Salthammer, T., Waring, M.S., Wierzbicka, A., 2017. Airborne particles in indoor environment of homes, schools, offices and aged care facilities: The main routes of exposure. Environ. Int. 108, 75–83. https://doi.org/10.1016/j.envint.2017.07.025

Morris, C.E., Sands, D.C., Bardin, M., Jaenicke, R., Vogel, B., Leyronas, C., Ariya, P.A., Psenner, R., 2011. Microbiology and atmospheric processes: research challenges concerning the impact of airborne micro-organisms on the atmosphere and climate. Biogeosciences 8, 17–25. https://doi.org/10.5194/bg-8-17-2011

Nathu, V.D., Virkutyte, J., Rao, M.B., Nieto-Caballero, M., Hernandez, M., Reponen, T., 2022. Direct-Read Fluorescence-Based Measurements of Bioaerosol Exposure in Home Healthcare. Int. J. Environ. Res. Public. Health 19, 3613. https://doi.org/10.3390/ijerph19063613

National Environment Agency, 2021. Climate of Singapore [WWW Document]. URL http://www.weather.gov.sg/climate-climate-of-singapore/ (accessed 6.25.21).

Nazaroff, W.W., 2016. Indoor bioaerosol dynamics. Indoor Air 26, 61–78. https://doi.org/10.1111/ina.12174

Nazaroff, W.W., 2004. Indoor particle dynamics. Indoor Air 14, 175–183. https://doi.org/10.1111/j.1600-0668.2004.00286.x

Nieto-Caballero, M., 2021. GitHub repository: InstaScope [WWW Document]. URL https://github.com/marinanieto/InstaScope (accessed 2.17.22).

Nieto-Caballero, M., Gomez, O.M., Shaughnessy, R., Hernandez, M., 2021. Aerosol fluorescence, airborne hexosaminidase, and quantitative genomics distinguish reductions in airborne fungal loads following major school renovations. Indoor Air 32, e12975. https://doi.org/10.1111/ina.12975

Ong, T.C., 2005. Aerobiology, image analysis and allergenicity of pollen and spores in Singapore (Thesis). National University of Singapore, Singapore.

Patra, S.S., Wu, T., Wagner, D.N., Jiang, J., Boor, B.E., 2021. Real-time measurements of fluorescent aerosol particles in a living laboratory office under variable human occupancy and ventilation conditions. Build. Environ. 108249. https://doi.org/10.1016/j.buildenv.2021.108249

Perring, A.E., Schwarz, J.P., Baumgardner, D., Hernandez, M.T., Spracklen, D.V., Heald, C.L., Gao, R.S., Kok, G., McMeeking, G.R., McQuaid, J.B., Fahey, D.W., 2015. Airborne observations of regional variation in fluorescent aerosol across the United States. J. Geophys. Res. Atmospheres 120, 1153–1170. https://doi.org/10.1002/2014JD022495

Pitz, M., Schmid, O., Heinrich, J., Birmili, W., Maguhn, J., Zimmermann, R., Wichmann, H.-E., Peters, A., Cyrys, J., 2008. Seasonal and diurnal variation of PM2. 5 apparent particle density in urban air in Augsburg, Germany. Environ. Sci. Technol. 42, 5087–5093. https://doi.org/10.1021/es7028735

Pöhlker, C., Huffman, J.A., Pöschl, U., 2012. Autofluorescence of atmospheric bioaerosols – fluorescent biomolecules and potential interferences. Atmospheric Meas. Tech. 5, 37–71. https://doi.org/10.5194/amt-5-37-2012

Pöschl, U., Martin, S.T., Sinha, B., Chen, Q., Gunthe, S.S., Huffman, J.A., Borrmann, S., Farmer, D.K., Garland, R.M., Helas, G., Jimenez, J.L., King, S.M., Manzi, A., Mikhailov, E., Pauliquevis, T., Petters, M.D., Prenni, A.J., Roldin, P., Rose, D., Schneider, J., Su, H., Zorn, S.R., Artaxo, P., Andreae, M.O., 2010. Rainforest Aerosols as Biogenic Nuclei of Clouds and Precipitation in the Amazon. Science 329, 1513–1516. https://doi.org/10.1126/science.1191056

Prussin, A.J., Marr, L.C., 2015. Sources of airborne microorganisms in the built environment. Microbiome 3, 78. https://doi.org/10.1186/s40168-015-0144-z

Schwartz, D., Collins, F., 2007. Environmental biology and human disease. Science 316, 695–696. https://doi.org/10.1126/science.1141331

Shiraiwa, M., Ueda, K., Pozzer, A., Lammel, G., Kampf, C.J., Fushimi, A., Enami, S., Arangio, A.M., Fröhlich-Nowoisky, J., Fujitani, Y., Furuyama, A., Lakey, P.S.J., Lelieveld, J., Lucas, K., Morino, Y., Pöschl, U., Takahama, S., Takami, A., Tong, H., Weber, B., Yoshino, A., Sato, K., 2017. Aerosol Health Effects from Molecular to Global Scales. Environ. Sci. Technol. 51, 13545–13567. https://doi.org/10.1021/acs.est.7b04417

Smith, M., Matavulj, P., Mimić, G., Panić, M., Grewling, Ł., Šikoparija, B., 2022. Why should we care about high temporal resolution monitoring of bioaerosols in ambient air? Sci. Total Environ. 826, 154231. https://doi.org/10.1016/j.scitotenv.2022.154231

Strak, M., Janssen, N.A.H., Godri, K.J., Gosens, I., Mudway, I.S., Cassee, F.R., Lebret, E., Kelly, F.J., Harrison, R.M., Brunekreef, B., Steenhof, M., Hoek, G., 2012. Respiratory Health Effects of Airborne Particulate Matter: The Role of Particle Size, Composition, and Oxidative Potential—The RAPTES Project. Environ. Health Perspect. 120, 1183–1189. https://doi.org/10.1289/ehp.1104389

Tian, Y., Liu, Y., Misztal, P.K., Xiong, J., Arata, C.M., Goldstein, A.H., Nazaroff, W.W., 2018. Fluorescent biological aerosol particles: Concentrations, emissions, and exposures in a northern California residence. Indoor Air 28, 559–571. https://doi.org/10.1111/ina.12461

Toivola, M., Nevalainen, A., Alm, S., 2004. Personal exposures to particles and microbes in relation to microenvironmental concentrations. Indoor Air 14, 351–359. https://doi.org/10.1111/j.1600-0668.2004.00258.x

Wang, P., Liu, J., Wang, C., Zhang, Z., Li, J., 2022. A holistic performance assessment of duct-type electrostatic precipitators. J. Clean. Prod. 357, 131997. https://doi.org/10.1016/j.jclepro.2022.131997

Wei, K., Zou, Z., Zheng, Y., Li, J., Shen, F., Wu, C., Wu, Y., Hu, M., Yao, M., 2016. Ambient bioaerosol particle dynamics observed during haze and sunny days in Beijing. Sci. Total Environ. 550, 751–759. https://doi.org/10.1016/j.scitotenv.2016.01.137

World Health Organization, 2021. WHO global air quality guidelines: particulate matter (PM2.5 and PM10), ozone, nitrogen dioxide, sulfur dioxide and carbon monoxide.

Wu, T., Täubel, M., Holopainen, R., Viitanen, A.-K., Vainiotalo, S., Tuomi, T., Keskinen, J., Hyvärinen, A., Hämeri, K., Saari, S.E., Boor, B.E., 2018. Infant and Adult Inhalation Exposure to Resuspended Biological Particulate Matter. Environ. Sci. Technol. 52, 237–247. https://doi.org/10.1021/acs.est.7b04183

Wu, X. (May), Apte, M.G., Bennett, D.H., 2012. Indoor particle levels in small-and medium-sized commercial buildings in California. Environ. Sci. Technol. 46, 12355–12363. https://doi.org/10.1021/es302140h

Wu, Y., Chen, A., Luhung, I., Gall, E.T., Cao, Q., Chang, V.W.-C., Nazaroff, W.W., 2016. Bioaerosol deposition on an air-conditioning cooling coil. Atmos. Environ. 144, 257–265. https://doi.org/10.1016/j.atmosenv.2016.09.004

Xia, T., Qi, Y., Dai, X., Liu, Jinyu, Xiao, C., You, R., Lai, D., Liu, Junjie, Chen, C., 2021. Estimating long-term time-resolved indoor PM2.5 of outdoor and indoor origin using easily obtainable inputs. Indoor Air 31, 2020–2032. https://doi.org/10.1111/ina.12905

Yamamoto, N., Hospodsky, D., Dannemiller, K.C., Nazaroff, W.W., Peccia, J., 2015. Indoor Emissions as a Primary Source of Airborne Allergenic Fungal Particles in Classrooms. Environ. Sci. Technol. 49, 5098–5106. https://doi.org/10.1021/es506165z

Yang, S., Bekö, G., Wargocki, P., Williams, J., Licina, D., 2020. Human Emissions of Size-Resolved Fluorescent Aerosol Particles: Influence of Personal and Environmental Factors. Environ. Sci. Technol. acs.est.0c06304. https://doi.org/10.1021/acs.est.0c06304

Ye, J., Qian, H., Zhang, J., Sun, F., Zhuge, Y., Zheng, X., Cao, G., 2021. Concentrations and size-resolved I/O ratios of household airborne bacteria and fungi in Nanjing, southeast China. Sci. Total Environ. 774, 145559. https://doi.org/10.1016/j.scitotenv.2021.145559

Yin, P., Guo, J., Wang, L., Fan, W., Lu, F., Guo, M., Moreno, S.B.R., Wang, Y., Wang, H., Zhou, M., Dong, Z., 2020. Higher Risk of Cardiovascular Disease Associated with Smaller Size-Fractioned Particulate Matter. Environ. Sci. Technol. Lett. 7, 95–101. https://doi.org/10.1021/acs.estlett.9b00735

Yin, Y., He, J., Zhao, L., Pei, J., Yang, X., Sun, Y., Cui, X., Lin, C.-H., Wei, D., Chen, Q., 2022. Identification of key volatile organic compounds in aircraft cabins and associated

inhalation health risks. Environ. Int. 158, 106999. https://doi.org/10.1016/j.envint.2021.106999

Zhou, J., Fang, W., Cao, Q., Yang, L., Chang, V.W.-C., Nazaroff, W.W., 2017. Influence of moisturizer and relative humidity on human emissions of fluorescent biological aerosol particles. Indoor Air 27, 587–598. https://doi.org/10.1111/ina.12349

Zuraimi, M.S., 2010. Is ventilation duct cleaning useful? A review of the scientific evidence: Ventilation duct cleaning review. Indoor Air 20, 445–457. https://doi.org/10.1111/j.1600-0668.2010.00672.x

Zuraimi, M.S., Magee, R., Nilsson, G., 2012. Development and application of a protocol to evaluate impact of duct cleaning on IAQ of office buildings. Build. Environ. 56, 86–94. https://doi.org/10.1016/j.buildenv.2012.02.008

Zuraimi, M.S., Li, J., Pantelic, J., Schiavon, S., 2022. Indoor air pollution of outdoor origin: mitigation using portable air cleaners in Singapore office building. Aerosol Air Qual. Res. In-press.